Bicycle Wheel System Identification and Optimal Truing Control for Mechatronic Systems

Aaron Hunter

***Abstract*—Put your abstract here**

***Index Terms*—IEEE, IEEEtran, journal.**

I. Introduction

THE spoked bicycle wheel is one of the most ubiquitous tensioned structures in the world. While much has been written about modeling the structure itself (reference Ford's thesis for a good literature review) very little has been published regarding the assembly and tuning of the structure itself. This work presents a framework for a rigorous approach to empirically modeling a bicycle wheel and provides for an optimal tensioning method for all wheels of the same type. This framework is intended for integration into a mechatronic wheel manufacturing apparatus although the results presented here were produced by hand, albeit with the assistance of measurement sensors and a computer.

Our approach builds upon the one proposed by Papadapolous (cite patent) and alluded to in (cite Holland patent) for the wheel tensioning method. This approach is to measure the influence of a tension adjustment to a spoke on the lateral, radial, and tension parameters of a specific wheel. These influence functions are generated for each spoke and input into a model in matrix form. This model is then employed to compute a weighted least squares estimation of the tension adjustments that minimize the wheel parameter variations for a given wheel under tensioning. Where this work improves upon previous approaches is to provide tension targeting and a method for feedback control during the tensioning process to minimize cumulative adjustment errors.

II. Background

The bicycle wheel structure consists of a rim, spokes, spoke nipples, and a hub (see figure of wheel). The hub anchors the spoke which is connected to the rim by a nippled threaded onto its end. The nipple is seated in the rim. The wheel stiffness is generated by providing tension to the spokes by tightening the nipples until the desired tension is achieved. Lateral stiffness of the wheel is provided by the lateral component of the spoke tension due to the spoke angle α in fig(cite fig here). Lateral stiffness prevents rim warping and allows for adjustment of lateral variations. Radial stiffness is provided by the radial component of the spoke tension and allows for compensating for radial variations. The optimal tension of the wheel is a balance between the two–high enough tension to support the anticipated load, but below the value that begins to induce rim warpage (cite Ford here).

Spoking patterns vary from purely radial to nearly tangential relative to the hub and determined by angle β. Tangential spoke patterns allow for torque transmission from the hub to the rim, as occurs through the drive train or from disc brakes, so most wheels have some tangential component, the exception being front wheels with rim brakes.

The process of adjusting the tension to minimize the lateral and radial variations of the wheel is called truing. The typical procedure for wheel truing by hand is a heuristic where first the average spoke tension is applied, then the lateral variations are iteratively reduced, and finally the radial variations are minimized. The wheel tension is then increased incrementally and the procedure is repeated until the wheel parameter specifications are met (cite Brandt).

The wheel can be modeled as a system of springs operating in a linear regime (Ford again). Because of this linear property, the wheel parameter variations induced by a set of spokes can be decomposed into superposed individual spoke tensions, lending itself to least squares analysis developed in the next sections.

III. Apparatus

To develop the model a symmetric (i.e., tensioned equally on both sides), front wheel was built by hand using a Stans ZTR Alpha rim, a White Industries MI5 hub, and 32 DT Swiss Competition spokes. A so-called 'three-cross' tangential spoke pattern was employed for the wheel geometry. All adjustments were performed on a Centrimaster Comfort wheel truing stand. This stand has radial and lateral mechanical dial gauges to measure the rim displacements with 0.1 mm gauge markings. To obtain optimal resolution and to minimize measurement time, a Canon EOS M digital camera with a 22mm focal length lens was used to capture images from the dial gauges. A computer vision algorithm was used to analyze the images and calculate the displacements. Finally, a WheelFanatyk digital tension gauge was used to measure spoke tension. This instrument measures displacement of the spoke under a known spring tension. This displacement is converted to a measured tension based on a lookup table provided by the manufacturer. It has an accuracy of 10 % and the measurements are discretized to 0.01 mm.

IV. Method

A. Wheel Model

The approach taken here is to determine the effect of a unit change in spoke tension on the lateral, radial and tension

A. Hunter is a PhD student at the Department of Computer Science and Engineering, University of California, Santa Cruz, CA, 95054 USA e-mail: aamuhunt@ucsc.edu.

Manuscript received April 19, 2005; revised August 26, 2015.

Fig. 1. Apparatus used to measure wheel properties

parameters of a wheel as measured as a function of rim angle as illustrated in fig(). The resulting curves are referred to as the influence functions of the spoke. To find these influence functions a series of experiments are performed on a subset of the spokes in a given wheel. For each experiment a spoke is loosened by one complete rotation and measurements are taken equal increments along the rim for the radial and lateral displacements and tension measurements are taken for every spoke. The data are used to develop the influence functions, either as a discrete sequence or fit to the Fourier series. The influence functions for each spoke are then placed into matrix forms such that each column represents the influence of a given spoke and each row represents a discrete rim angle. In other words, if $u_s(\theta), v_s(\theta),$ and $t_s(\theta)$ are the lateral and radial influence functions for spoke $s \in [1, 2, \cdots, n_s]$, then the influence matrices Φ_u, Φ_v and Φ_t for the lateral, radial and tension parameters respectively, at the discrete rim angles $\theta \in [\theta_1, \theta_2, \cdots, \theta_n]$ are given by:

$$\mathbf{u_s} = \begin{bmatrix} u_s(\theta_1) \\ u_s(\theta_2) \\ \vdots \\ u_s(\theta_n) \end{bmatrix} \mathbf{v_s} = \begin{bmatrix} v_s(\theta_1) \\ v_s(\theta_2) \\ \vdots \\ v_s(\theta_n) \end{bmatrix} \mathbf{t_s} = \begin{bmatrix} t_s(\theta_1) \\ t_s(\theta_2) \\ \vdots \\ t_s(\theta_n) \end{bmatrix}$$

$$\begin{aligned} \Phi_u &= \begin{bmatrix} \mathbf{u_1} & \mathbf{u_2} & \dots & \mathbf{u_{n_s}} \end{bmatrix} \\ \Phi_v &= \begin{bmatrix} \mathbf{v_1} & \mathbf{v_2} & \dots & \mathbf{v_{n_s}} \end{bmatrix} \\ \Phi_t &= \begin{bmatrix} \mathbf{t_1} & \mathbf{t_2} & \dots & \mathbf{t_{n_s}} \end{bmatrix} \end{aligned}$$

The influence matrices are the models of the wheel for each parameter. We combine these matrices into a single matrix Φ:

$$\Phi = \begin{bmatrix} \Phi_u \\ \Phi_v \\ \Phi_t \end{bmatrix} \tag{1}$$

Given a vector of tension adjustments (i.e., rotations of the spoke nipples), $\mathbf{d}$, the prediction of the wheel state after applying the adjustments is given by:

$$\hat{\mathbf{Y}} = \mathbf{Y_b} + \Phi\mathbf{d} \tag{2}$$

where $\hat{\mathbf{Y}}$ is the predicted state of the wheel after tensioning and $\mathbf{Y_b}$ is the state of the wheel prior to tensioning.

To find the optimal vector of spoke tension adjustments $\mathbf{d}_{ls}$ that result in a measured state relative to a perfect wheel at average tention $\bar{T}$ we set up a weighted least squares approximation using a set of measurements $[\mathbf{u}, \mathbf{v}, \mathbf{T} - \bar{T}]$, and the weights μ_v and μ_t:

$$\tilde{\Phi} = \begin{bmatrix} \Phi_u \\ \Phi_v\sqrt{\mu_v} \\ \Phi_t\sqrt{\mu_t} \end{bmatrix} \quad \tilde{\mathbf{Y}} = \begin{bmatrix} \mathbf{u} - u_0 \\ (\mathbf{v} - v_0)\sqrt{\mu_v} \\ (\mathbf{T} - \bar{T})\sqrt{\mu_t} \end{bmatrix}$$

$$\mathbf{d}_{ls} = \tilde{\Phi}^{\dagger}\tilde{\mathbf{Y}} \tag{3}$$

Where $\tilde{\Phi}^{\dagger}$ is the pseudo-inverse of $\tilde{\Phi}$. Typically u_0 and v_0 are zero reflecting the fact that the gauge has been set to zero at the desired lateral and radial locations during setup. The weighting factors represent the tradeoff between the lateral, radial, and tension variables and account for the difference in units, the quality of measurements, as well as the specification for each parameter. We will determine the weighting factors through simulation and validate them experimentally. Once $\mathbf{d}_{ls}$ is found the wheel is trued to its optimal state, $\hat{\mathbf{Y}}_{ls}$ by applying $\mathbf{d}_{adj} = -\mathbf{d}_{ls}$ to the wheel:

$$\hat{\mathbf{Y}}_{ls} = \mathbf{Y_b} + \Phi\mathbf{d}_{adj} \tag{4}$$

B. Tension Targeting

In theory adjusting a wheel to any arbitrary average tension is accomplished by setting $\bar{T} = T_d$, where T_d is the desired tension. In practice however, the tension influence functions are noisy and lack the necessary precision to target tension accurately. However, we can exploit the wheel symmetry to make the following observation. For a symmetric wheel, if every spoke is tightened by the same amount then the radial and lateral displacements are unaffected and only the mean tension is changed. It is possible therefore to decouple the average tension change from spoke tension non-uniformity. It should be apparent that this is possible for asymmetric wheels as well, such as a drive wheel or wheel with a disc brake, by compensating for the different spoke angles.

Our approach is as follows. We calculate $\mathbf{d}_{ls}$ as in (**??**) and subtract its mean value:

$$\mathbf{d} = -(\mathbf{d}_{ls} - \bar{d}_{ls})$$

If we apply $\mathbf{d}$ to a wheel it will minimize lateral, radial and tension variations as before, but without affecting the average tension. We then calculate the necessary constant shift d_{cm} to bring the average tension to T_d:

$$d_{cm} = (T_d - \bar{T})/c$$

Where the proportionality constant, c, is determined experimentally. The spoke vector that will optimally true the wheel becomes:

$$\mathbf{d}_{adj} = \mathbf{d} + d_{cm} \tag{5}$$

C. Optical Digitization

The method for converting the analog dial gauge readings into digital measurements merits some discussion. Although a mechatronic implementation of a wheel tensioning machine would likely use digital gauges, it is instructive to demonstrate the effectiveness of optical digitization. Prior to taking measurements two images are collected. The first is a reference image taken with the gauge needles outside the range of expected data range. The second image is taken with the needles set to zero. With these two images any subsequent image of a measurement is processed in the following manner. The measurement image is subtracted from the reference image after appropriate smoothing. If the images are taken under the same conditions, what remains after subtraction is a ghost image of the needles themselves. A binary threshold is applied to the subtracted image and masked. Finally, the centroid of the needle tip is determined and an angle from the gauge center to the tip is calculated and compared to the measurement at zero. The angle is then converted into displacement using the gauge resolution. This process is shown in Fig().

D. Wheel Truing Algorithm

Having determined the optimal spoke adjustments, $\mathbf{d}_{adj}$, the remaining task is to apply them to the wheel. Although this sounds deceptively simple, there are some difficulties doing this accurately. The main one is a problem of spoke twist. Spokes are not torsionally stiff and will twist significantly during nipple rotation. Thus it is difficult to precisely determine how far the spoke nipple has been adjusted based entirely on the rotation angle of the spoke nipple. The servo accuracy or precision may also be inadequate, leading to the accumulation of errors over multiple spoke adjustments. This is particularly true at higher spoke tensions where the friction of the nipple-spoke interface can lead to discrete jumps in nipple rotation. Finally, even if the nipple has been adjusted properly but the spoke is twisted, over time it can un-twist which may result in tension loss of the spoke and causing the wheel to go out of true.

Although the use of high precision servos and clamping the spoke during adjustment improve the wheel truing process, we have developed a method which minimize these sources of variability using lateral feedback during each spoke adjustment. The method begins with the first element of $\mathbf{d}_{adj}$. Using (2) the post-adjustment lateral displacement at the rim angle of that spoke is predicted as the target displacement. The spoke tension is then adjusted until the lateral measurement equals the target displacement. Spoke twist is then eliminated by measuring the spoke rotation hysteresis and setting the spoke nipple angle midway in the hysteresis regime. Note that this lateral target is not zero, but rather the intermediate state of the wheel after the adjustment of the first spoke. Then a prediction is made of the lateral state at the rim angle of the second spoke after the first *two* adjustments have been performed. The second spoke tension is adjusted until the target is reached in the same manner of the first. This process continues sequentially for every element in $\mathbf{d}_{adj}$. This method minimizes any accumulation of adjustment error while eliminating spoke twist. Fig(2) shows the intermediate lateral states of a wheel undergoing this method along with the lateral targets for each spoke adjustment.

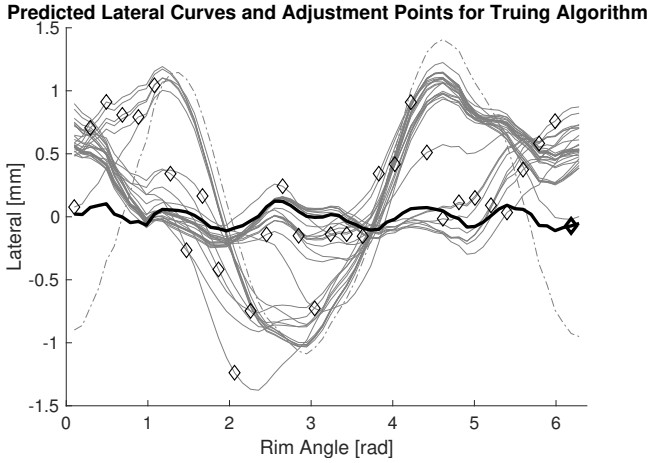

Fig. 2. Example of the truing algorithm. The dashed line is the baseline lateral state. The thin lines are the predicted states after each spoke adjustment. The spoke tension is adjusted until the lateral measurement equals the diamond target and proceeds from the first spoke (leftmost) to the last. The thick line is the predicted final state with its truing target.

V. Results

A. Optical Digitization of Lateral and Radial Measurements

To provide for higher precision measurements and to automate analog to digital conversion of the analog dial gauge measurements a computer vision algorithm was employed. To validate the measurement reliability a series of four images were taken. They were first analyzed for their readings manually (through pixel level measurement of the angle of the needles) and then compared against the results returned by the algorithm. Both dial gauges were set to approximately the following settings: 1.0 mm, 0.5 mm, 0.25 mm, and 0.0 mm. Fig(3) shows the comparison between the two methods. The estimated effective displacement resolution of the manual measurement method is approximately 0.014 mm. The computer vision algorithm returned values within ± 0.007 mm of the manual measurements.

B. Influence Curves

The influence curves for the lateral and radial displacements were taken at 64 equally spaced locations on the rim–at each spoke and halfway between each spoke. 32 curves were measured, one for each spoke in the wheel. These curves were averaged and in the case of the radial displacement, the mean value subtracted (for our purposes the rim is considered incompressible in the tangential direction, thus a tension change should not induce an average radial change). The subsequent influence curves are shown in Fig(4). The tension influence curves were measured for each spoke. This particular spoking geometry results in four distinct tension curves, depending on whether the spoke is on the drive side of the wheel, or the non-drive side, and whether it is a 'leading' spoke or a

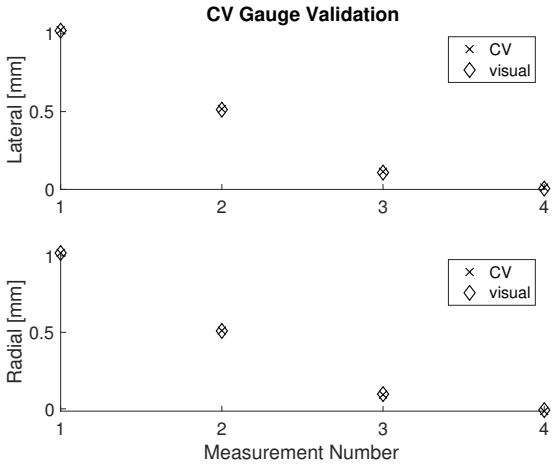

Fig. 3. Validation of the computer vision algorithm developed to interpret analog dial gauge measurements. Both the lateral and radial dials were set to approximately 1, 0.5, 0.25, and 0.0mm. The measurements were interpreted through visual estimation of the images as well as by the algorithm. The results agree to better than the estimate of the resolution of the manual technique.

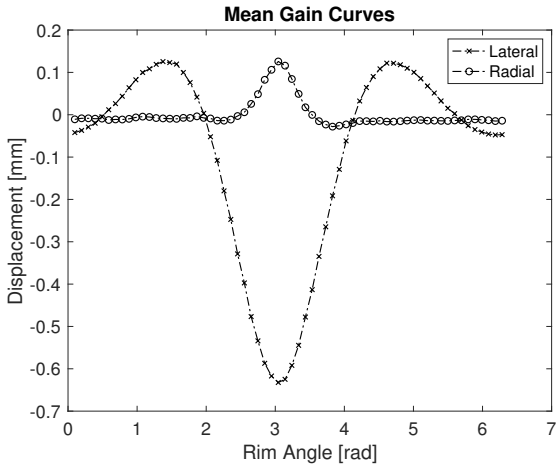

Fig. 4. The mean influence curves for the lateral and radial parameters. These curves are the average of 32 measured curves.

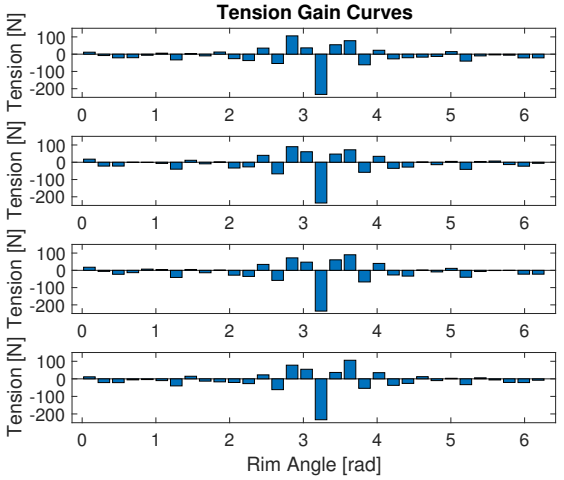

Fig. 5. The mean influence curves for spoke tension. From top to bottom: (a) Non-drive side leading. (b) Drive-side leading. (c) Non-drive side trailing. (d) Drive side trailing. Note that (a) and (d) are mirror images, as are (b) and (c).

'trailing' spoke, that is whether its spoke angle, β, is positive or negative (see Fig()). Because this is a symmetric wheel, however, the non-drive side leading spoke influence curve is a mirror image of the drive side trailing one. Similarly, the non-drive side trailing spoke influence curve is a mirror image of the drive side leading one. This symmetry was exploited to generate the four tension influence curves in Fig(5), such that each curve represents the average of 16 curves and is mirrored when necessary.

The lateral and radial influence curves can be used directly and put into the influence matrices. Alternatively, they can be fit to the Fourier series. The Fourier series is an ideal modeling method for these curves due to their continuous nature and 2π periodicity. The tension measurements are inherently discrete, however, so modeling them in this manner, while feasible, is not useful as the model requires as many terms as there are measurement for fidelity. There are analytical models available (cite Ford again), however, they require extensive characterization of the rim that is not possible *in-situ*. Therefore, for this work only the smoothed data were used for the influence matrices.

C. Simulation

With the influence matrices developed as in (1) the state of the wheel can be predicted for a given set of spoke tension adjustments. To find acceptable values for the weighting factors, μ_v, μ_t, a series of simulations were performed. For each simulation a random vector of spoke adjustments was generated and a wheel state prediction was calculated using (2). To this wheel state white noise was added to simulate the uncertainty of the measurement. The noise distributions were determined from the measured profiles generated during the influence curve development. The initial weighting factors were developed based on a comparison of the magnitude of the changes induced by a unit disturbance of the three parameters, normalized to the maximum lateral displacement. The weighted least squares estimation of the random spoke vector was then computed using these weighting factors and (3). and the predicted final state of the wheel is calculated using (4). The weighting factors were then modified until both the predicted performance of the algorithm met a specification of $\pm$ 0.1mm in lateral and radial error and $\pm$50 N in tension error relative to a perfectly true wheel. The predicted spoke vector is generally found to agree to an rms of $\leq$ 0.1 revolutions. Fig(6) shows the result of one such simulation. After extensive simulation acceptable weighting factors were found to be: $\mu_v = 0.5$, $\mu_t = 10^{-5}$.

D. Model Validation

The model is separated into two parts, spoke adjustments which affect the variation of the three wheel parameters around a mean value, and adjustments which affect the mean tension. The latter part of the model is found by determining the coefficient, c between the average of the spoke adjustment

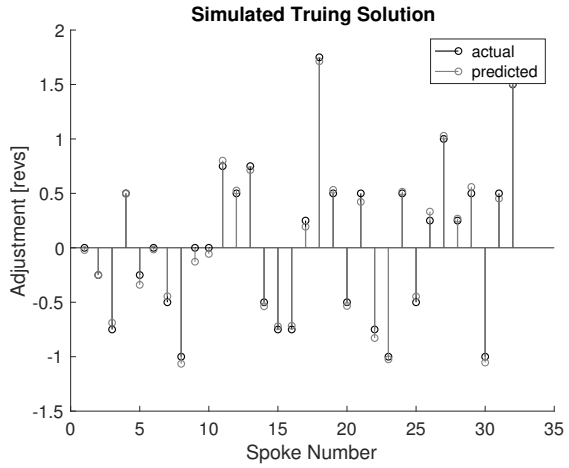

Fig. 6. The actual and predicted spoke tensioning values used during a simulation of wheel truing. The prediction agrees with the actual values to an rms error of 0.05 revolutions.

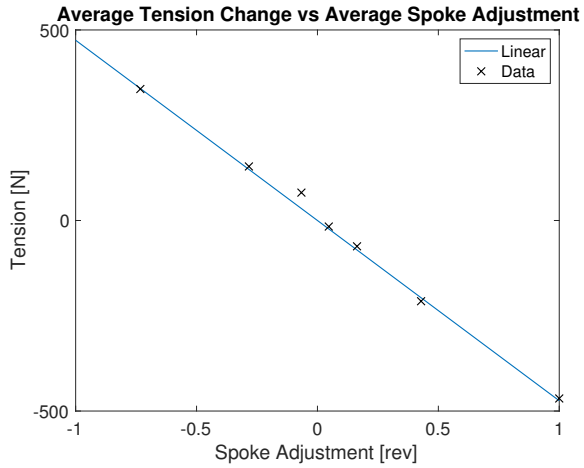

Fig. 7. The average tension change of a truing operation compared to the average of the spoke adjustment vector. A linear fit to the data finds $c = -473$.

vector and the average tension change of the wheel. Fig(7) demonstrates the results of seven experiments. A linear fit to these data finds $c = -473$. In practice, this constant could be derived from a single experiment where every spoke is adjusted by one revolution.

To validate the model performance for spoke adjustment vectors that cause changes of the wheel state other than mean tension, a different experiment was performed. In this case a random vector of spoke adjustments was applied to the (manually trued) test wheel and the resulting measured wheel parameters were compared to the model predictions. The truing algorithm was used to accurately make the spoke adjustments Fig(8) shows the result of this experiment and Fig(9) shows the residual error of model after the adjustment. The rms model error of the lateral, radial and tension parameters are found to be 0.123mm, 0.049mm, and 33N, respectively.

E. Wheel Truing Validation

To validate the complete model and truing algorithm the de-trued wheel from the previous experiment was trued to a

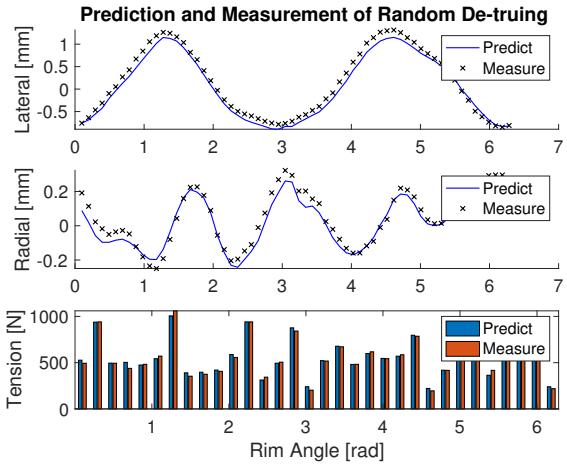

Fig. 8. The actual and predicted lateral, radial, and tension values for the random de-truing experiment.

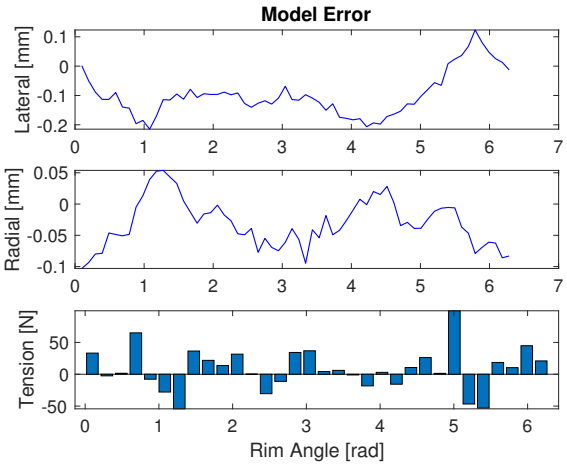

Fig. 9. The model error relative to the measurements for the random de-truing experiment. The rms errors are found to be 0.123 mm (lateral), 0.049 mm (radial), and 33 N (tension).

TABLE I
TRUING ALGORITHM RESULTS

Parameter	Inital ($\mu \pm \sigma$)	Final ($\mu \pm \sigma$)
Lateral [mm]	0.160 ± 0.736	-0.037 ± 0.107
Radial [mm]	0.050 ± 0.158	-0.046 ± 0.047
Tension [N]	556 ± 211	1009 ± 45

target tension of 1000 N. Fig(10) shows the wheel state before and after the truing operation and Table(I) summarizes the measurements. The maximum variations are 0.17 mm above the mean (lateral), 0.07 mm above the mean (radial), and 104 N below the mean (tension).

Finally, to see whether the performance of the truing algorithm could improve the wheel from the truing experiment was trued again. The results are shown in Table(II). The performance is modestly improved for every parameter.

VI. CONCLUSION

The conclusion goes here.

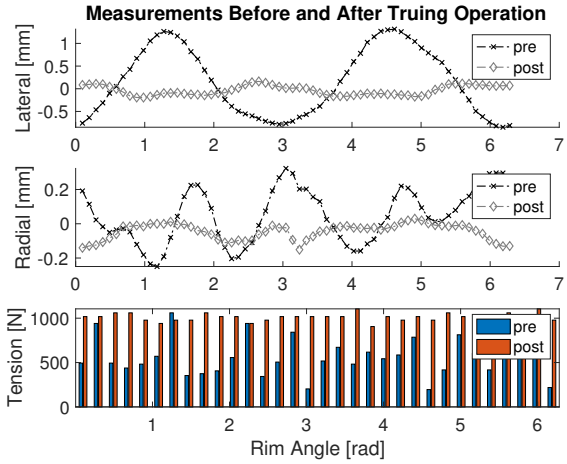

Fig. 10. The state of the wheel is shown before and after the truing operation. The results are summarized in the text.

TABLE II
SECOND ITERATION OF TRUING

Parameter	Inital ($\mu \pm \sigma$)	Final ($\mu \pm \sigma$)
Lateral [mm]	-0.037 ± 0.107	0.028 ± 0.073
Radial [mm]	-0.046 ± 0.047	-0.031 ± 0.034
Tension [N]	1009 ± 45	989 ± 39

ACKNOWLEDGMENT

The authors would like to thank...

REFERENCES

[1] H. Kopka and P. W. Daly, *A Guide to LaTeX*, 3rd ed. Harlow, England: Addison-Wesley, 1999.

PLACE PHOTO HERE

Michael Shell Biography text here.

John Doe Biography text here.

Jane Doe Biography text here.